Stability and equation of state of the post-perovskite phase in $MgGeO_3$ to 2 Mbar

Atsushi Kubo,[1] Boris Kiefer,[2] Guoyin Shen,[3,4] Vitali B. Prakapenka,[3] Robert J. Cava,[5] and Thomas S. Duffy[1]

Received 5 January 2006; revised 27 March 2006; accepted 12 April 2006; published 27 May 2006.

[1] The stability and equation of state of the post-perovskite phase in $MgGeO_3$ were investigated to 2 Mbar by in situ x-ray diffraction experiments using the laser-heated diamond cell as well as by theoretical calculations using density functional theory. The stability of the phase was demonstrated at 92-201 GPa during laser heating. By using the Birch-Murnaghan equation of state, we obtained a zero-pressure volume (V_0) of 179.2 ± 0.7 Å^3, bulk modulus (K_0) of 207 ± 5 GPa with a pressure derivative (K'_0) of 4.4 from experiments at room temperatures, and V_0 = 178.02 Å^3, K_0 = 201.9 GPa, K'_0 = 4.34 from theoretical calculations at 0 K. The relative axial compressibilities of the silicate and germanate post-perovskite phases are similar although $MgSiO_3$ is more anisotropic than $MgGeO_3$.
Citation: Kubo, A., B. Kiefer, G. Shen, V. B. Prakapenka, R. J. Cava, and T. S. Duffy (2006), Stability and equation of state of the post-perovskite phase in $MgGeO_3$ to 2 Mbar, *Geophys. Res. Lett.*, *33*, L12S12, doi:10.1029/2006GL025686.

1. Introduction

[2] Since the discovery of the post-perovskite phase (pPv) in $MgSiO_3$ by *Murakami et al.* [2004], numerous studies of this phase have been carried out by theory and experiment [e.g., *Tsuchiya et al.*, 2004; *Oganov and Ono*, 2004; *Shim et al.*, 2004; *Mao et al.*, 2004; *Stackhouse et al.*, 2005]. There has also been strong interest in understanding the occurrence and properties of the pPv phase in other systems [e.g., *Caracas and Cohen*, 2005; *Tateno et al.*, 2006].

[3] Over the last 40 years, the crystal structures of germanates have been extensively examined as a low-pressure model for silicate structures [e.g., *Ringwood and Seabrook*, 1963]. Germanates have also been used as silicate analogs in studies of phase equilibria and thermodynamics [*Ross and Navrotsky*, 1988; *Akaogi et al.*, 2005], equation of state [*Sato et al.*, 1977], and elasticity [*Liebermann*, 1975]. In recent years, there has been emphasis on the use of germanates as analogs for the study of phase transformation mechanisms and kinetics, rheology, and microstructure development, especially in the Mg_2SiO_4 system [e.g., *Riggs and Green*, 2005]. Recently, *Hirose et al.* [2005] demonstrated that the pPv phase could be synthesized in $MgGeO_3$ composition at ~50 GPa lower than the transition pressure for $MgSiO_3$, suggesting that germanate could be a useful analog to study the physical properties of silicate pPv phase. Also, the first study of deformation behavior of $MgGeO_3$ pPv was recently reported [*Merkel et al.*, 2006]. Here we report experimental and theoretical results on stability, equation of state, and axial compressibilities of $MgGeO_3$ pPv phase to 2 Mbar. Our results expand upon earlier measurements [*Hirose et al.*, 2005] due to extended pressure range, use of soft pressure-transmitting media, and combination with first-principles calculations.

2. Experiment

[4] $MgGeO_3$ orthoenstatite was synthesized from a mixture of MgO (periclase) + GeO_2 (quartz) by heating in air at 1000 °C for 40 hours. Powder x-ray diffraction showed orthoenstatite with minor amounts of excess GeO_2. The sample was mixed with Pt (weight ratio of 8:2) which served as both a pressure standard and laser absorber.

[5] A symmetric diamond cell with Re gasket was used to generate high pressure. Three experimental runs were conducted. For run 1, the sample was insulated by Ar. In run 2, NaCl served as an insulating medium while for the third run $MgGeO_3$ unmixed with Pt was used as insulation.

[6] High-pressure x-ray diffraction experiments were carried out at 13-ID-D of the GSECARS sector at the Advanced Photon Source (APS). A monochromatic x-ray beam of 0.3344-Å wavelength was focused to a size of ~6 × 6 μm^2. An angle dispersive geometry with an image plate or CCD detector was employed. The detector was calibrated using CeO_2. We heated the samples from both sides using a TEM_{00} Nd:YLF laser. Temperature was measured by spectroradiometry. A complete description of the diamond cell high-pressure research facility at GSECARS can be found elsewhere [*Shen et al.*, 2005].

[7] Two-dimensional x-ray images were converted to one-dimensional diffraction patterns using Fit2d [*Hammersley et al.*, 1996]. Pressure was determined based on the equation of state of Pt by *Holmes et al.* [1989], which is known to give the highest pressure value relative to the other pressure scales for Pt and Au [*Akahama et al.*, 2002]. Lattice parameters of the pPv phase were calculated from the 020, 002, 022, 110, and 132 diffraction lines. Pressure-volume (P-V) data were fit using a third-order Birch-

[1]Department of Geosciences, Princeton University, Princeton, New Jersey, USA.
[2]Department of Physics, New Mexico State University, Las Cruces, New Mexico, USA.
[3]Consortium for Advanced Radiation Sources (CARS), University of Chicago, Argonne National Laboratory, Argonne, Illinois, USA.
[4]Now at High Pressure Collaborative Access Team (HPCAT), Advanced Photon Source, Argonne National Laboratory, Argonne, Illinois, USA.
[5]Department of Chemistry, Princeton University, Princeton, New Jersey, USA.

0094-8276/06/2006GL025686$05.00

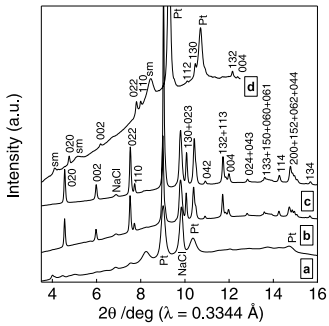

Figure 1. X-ray diffraction patterns at (a) 85 GPa prior to initial heating, (b) 92 GPa and 1740 K, (c) 89 GPa after heating, and at (d) 159 GPa after heating. Figures 1a–1c are from run 2 and Figure 1d from run 3. All *hkl* belong to pPv. NaCl, B2-phase; Pt, platinum; sm, starting material. The peaks from sm in Figure 1d are due to use of $MgGeO_3$ orthoenstatite as insulation.

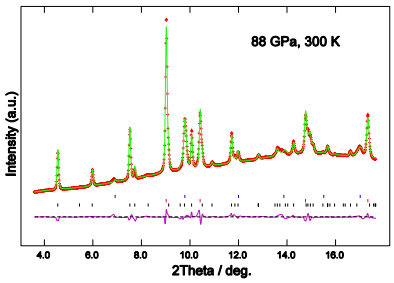

Figure 2. Rietveld refinement result. The crosses represent observed intensities (I_{obs}). The solid line is the calculated intensities (I_{calc}). The tick marks show the positions of calculated diffraction lines: upper ticks, NaCl (B2-phase); middle ticks, Pt: lower ticks, pPv. The line below the tick marks is the intensity difference curve ($I_{obs} - I_{calc}$).

Murnaghan equation of state to obtain the bulk modulus (K_0), its pressure derivative (K'_0), and zero-pressure unit cell volume (V_0). Linear compressibilities were determined from a modified Birch-Murnaghan equation [*Xia et al.*, 1998].

[8] Rietveld refinement was performed using GSAS [*Larson and Von Dreele*, 1994]. We refined lattice parameters, peak shape parameters, phase fractions, atomic positions, averaged displacement parameters, and spherical-harmonic terms in preferred orientation function.

[9] We also carried out first-principle calculations based on density functional theory (DFT) [*Hohenberg and Kohn*, 1964] using VASP [*Kresse and Hafner*, 1993; *Kresse and Furthmüller*, 1996] with the projector-augmented-wave method [*Kresse and Joubert*, 1999]. Electronic correlations were treated within the local density approximation (LDA). Converged solutions to the Kohn-Sham equations were obtained with energy-cutoff of 600 eV and a 6x4x6 k-point grid. Total energies were converged to better than 2.3 meV/atom and Pulay stresses were less than 0.6 GPa.

3. Results and Discussion

[10] Samples were initially compressed at room temperature to high pressures, where only weak and broad diffraction peaks were observed (Figure 1). In run 1, the sample at ~83 GPa was initially heated up to 1900 ± 300 K for ~4 minutes. After quenching, strong diffraction peaks of pPv phase ($CaIrO_3$-type structure, *Cmcm*) were observed. The sample was then compressed to ~95 GPa and heated to ~1700 K for 5 minutes, and further compressed up to 107 GPa and then decompressed in steps (see auxiliary material).[1] During decompression, the sample was not heated to avoid back transformation to low-pressure phases.

[11] In run 2, the sample was heated to ~1750 K for ~10 minutes at 92-95 GPa. Diffraction patterns obtained during and after heating are shown in Figures 1b and 1c. In this run, we obtained smooth Debye rings of pPv suitable for Rietveld method. The sample was decompressed to room pressure in steps without heating. Significant weakening and broadening of pPv peaks were observed beginning at 48 GPa. Diffraction peaks of the pPv phase were observed at 7 GPa but disappeared at room pressure.

[12] In run 3, we heated the sample to ~1600 K at 170 GPa for 5 minutes. Crystallization of the pPv phase was confirmed during heating, and the phase was quenched to 300 K at 159 GPa (Figure 1d). The sample was further compressed to 196 GPa, and diffraction peaks from the pPv phase were still observed during heating at ~1600 K at ~201 GPa for ~1 minute. Further measurements were not possible due to catastrophic failure of a diamond anvil.

[13] Rietveld refinement showed that the crystal structure of the pPv phase at 88 GPa is reasonably refined by the structure model of $CaIrO_3$-type (space group *Cmcm*) (Figure 2 and Table 1) in agreement with *Hirose et al.* [2005]. Table 1 also lists results obtained from DFT calculations. Atomic positions and lattice parameters are in good agreement with the Rietveld refinement.

[14] From the calculated enthalpy difference between Pv and pPv phases as a function of pressure, we predict that the pPv phase transition occurs at 45 GPa at 0 K without taking zero-point motion into account. This transition pressure is in agreement with that predicted by linear extrapolation of the phase boundary reported by *Hirose et al.* [2005] to 0 K.

[15] Analysis of deviatoric stress in Pt based on *Singh*'s [1993] method showed that the differential stress was 1–2 GPa during compression and 0–2 GPa during decompression. In this case, because of axial x-ray diffraction geometry employed in this study, pressures determined from diffraction lines of Pt are always underestimated. To reduce this systematic error, we used only 111 reflection of Pt to determine pressure since Pt has positive elastic anisotropy [*Kavner and Duffy*, 2003].

Table 1. Structural Parameters of $MgGeO_3$ pPv Phase From Rietveld Refinement and DFT Calculation

Method	Rietveld	DFT
P, GPa	87.8	86.3
a, Å	2.5964(3)	2.5943
b, Å	8.4113(9)	8.3856
c, Å	6.4059(6)	6.3853
Mg	0, 0.248(1), 0.25	0, 0.252, 0.25
Ge	0, 0, 0	0, 0, 0
O1	0, 0.928(2), 0.25	0, 0.915, 0.25
O2	0, 0.646(1), 0.440(2)	0, 0.642, 0.436

[1]Auxiliary material is available at ftp://ftp.agu.org/apend/gl/2006gl025686.

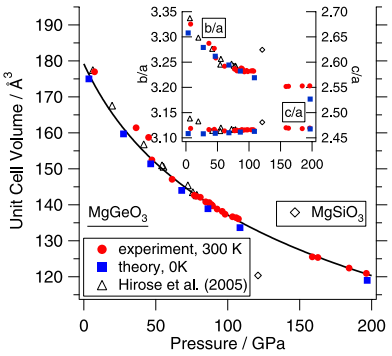

Figure 3. Pressure-volume data of $MgGeO_3$ and $MgSiO_3$ pPv phases. Compression curve is based on experimental results (see text). Inset shows variation of axial ratios versus pressure. Diamond symbols are after *Murakami et al.* [2004].

[16] Figure 3 shows our *P-V* data from experiments and DFT calculations together with previous results for $MgGeO_3$ and $MgSiO_3$. Average of the estimated standard deviation (1σ) in the experimentally-determined lattice parameters of the pPv phase is 0.11%. Experimental data obtained in three different runs above 47 GPa form a smooth trend, but data below 45 GPa tend to lie above this trend. As noted above, these lower pressure data exhibit broader peak widths and lower peak intensities. Such changes may reflect metastability of pPv phase and/or accumulation of deviatoric stress, both of which could yield larger unit cell volume. Therefore, we did not use data below 47 GPa for the equation of state analysis. Volumes obtained from DFT calculations are similar to but slightly lower than those from experiment which is typical for LDA calculations (Figure 3).

[17] Due to lack of data at low pressures (<47 GPa), it is difficult to simultaneously constrain V_0 and K_0 from our data set. We have therefore added a constraint from semi-empirical elasticity systematics ($K \cdot V$ = const. for a given crystal structure) [*Anderson and Anderson*, 1970]. As reference values, we used K_0 and V_0 of $MgSiO_3$ pPv at 0 K by theory and experiment (Table 2). By this method, we constrained equation of state parameters of $MgGeO_3$ pPv phase as $K_0 = 207 \pm 5$ GPa, $V_0 = 179.2 \pm 0.7$ Å^3 with fixed K_0' of 4.4 (solid line in Figure 3). Our DFT calculations at 0 K yielded $V_0 = 178.02$ Å^3, $K_0 = 201.9$ GPa, and $K_0' = 4.34$ for the pPv phase (Table 2). Our *P-V* data agree well with those reported by *Hirose et al.* [2005], but because they included the lower pressure data in the fitting, they obtained a larger V_0 and smaller K_0 (Table 2). If $K_0' = 4$, we obtain $K_0 = 245 \pm 5$ GPa and $V_0 = 175.9 \pm 0.6$ Å^3, showing significant trade-off between K_0 and K'_0 due to lack of data at low pressures.

[18] The Figure 3 inset shows axial ratios of the pPv phase. Average of the estimated standard deviation (1σ) in the experimentally-obtained axial ratios of the pPv phase is 0.09 % for *b*/*a* and 0.07 % for *c*/*a*. Although the *b*/*a* ratio decreases strongly with pressure at less than ~60 GPa, it becomes markedly less pressure dependent above 60 GPa. The *b*/a ratio becomes nearly constant at 70–110 GPa and 160–200 GPa with a step in between. Our theoretical calculations instead predict a smooth trend in *b*/*a*, and experiment and theory agree well to ~90 GPa. On the other hand, the trend of *c*/*a* is smooth and is also very consistent between experiments and theory.

Table 2. Equation of State Parameters of pPv Phases

Formula	V_0, Å^3	K_0, GPa	K_0'	Method[a]
$MgGeO_3$	179.2(7)	207 (5)	4.4	EXP, 1
$MgGeO_3$	183.1(8)	192 (5)	4.0	EXP, 2
$MgGeO_3$	178.02	201.9	4.34	DFT, 1
$MgSiO_3$	163.81(5)	222 (1)	4.2(1)	DFT, 3
$MgSiO_3$	162.86	231.9	4.43	DFT, 4
$(Mg,Fe)SiO_3$	164.9(6)	219 (5)	4.0	EXP, 5
$MgSiO_3$	162.86	225–249	4.0	EXP, 6

[a]EXP, experiment; DFT, first principles calculation; 1, This study; 2, *Hirose et al.* [2005]; 3, *Tsuchiya et al.* [2004]; 4, *Oganov and Ono* [2004]; 5, *Shieh et al.* [2006]; 6, *Ono et al.* [2006].

[19] Individual lattice parameters were fit using a modified form of the Birch-Murnaghan equation [*Xia et al.*, 1998]:

$$P = 3/2 \cdot K_{l0}\left[(l_0/l)^7 - (l_0/l)^5\right] \cdot \left\{1 + 3/4 \cdot \left(K'_{l0} - 4\right) \cdot \left[(l_0/l)^2 - 1\right]\right\}, \quad (1)$$

where l_0, K_{l0} and K'_{l0} are the zero-pressure length, incompressibility, and its pressure derivative of the *l*-axis ($l = a, b, c$), respectively. Least squares fitting yielded $K_{a0} = 230 \pm 4$ GPa, $a_0 = 2.803 \pm 0.002$ Å^3 with K'_{a0} of 4.6, $K_{b0} = 161 \pm 7$ GPa, $b_0 = 9.292 \pm 0.027$ Å^3 with K'_{b0} of 4.0, and $K_{c0} = 247 \pm 3$ GPa, $c_0 = 6.882 \pm 0.005$ Å^3 with K'_{c0} of 4.7. The linear compressibility of the *l*-axis, β_l, can be expressed as [*Xia et al.*, 1998]:

$$\beta_l = -1/l \cdot (\partial l/\partial P)_T = 1/(3K_l). \quad (2)$$

The calculated linear compressibilities are shown in Figure 4, demonstrating good agreement between experiments and theory. Also shown are results for $MgSiO_3$ from *Oganov and Ono* [2004] and *Stackhouse et al.* [2005], indicating similar behavior in axial compressibility between germanate and silicate pPv phases. However, $MgGeO_3$ pPv at 60–120 GPa is 10–15 % less anisotropic than $MgSiO_3$ pPv at 120 GPa in terms of β_b/β_c, implying that anisotropy of $MgGeO_3$ pPv in various physical properties may be less than that of $MgSiO_3$ pPv.

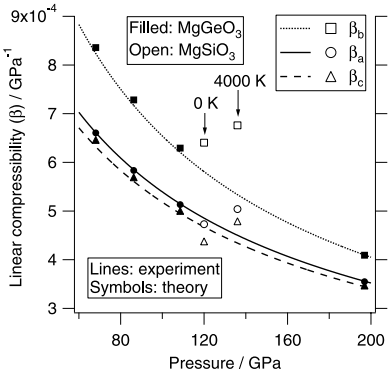

Figure 4. Linear compressibility of pPv phases. Open symbols at 0 K and 4000 K are by *Oganov and Ono* [2004] and *Stackhouse et al.* [2005], respectively.

[20] Based on the above results, we conclude that germanate could behave as a useful analog to silicate pPv phase because of lower transition pressure, stronger diffraction intensities, consistency in elasticity systematics, and generally similar behavior in axial compressibilities. We infer that the pPv phase in $MgSiO_3$ should be stable to a few megabars from the results of stability of $MgGeO_3$ pPv phase to 2 Mbar and pPv transition pressure in $MgGeO_3$ [*Hirose et al.*, 2005] that is ~60 GPa lower than that in $MgSiO_3$ [e.g., *Murakami et al.*, 2004].

[21] **Acknowledgments.** We thank Sofia Akber-Knutson, Sean R. Shieh and Claire E. Runge for their assistance and Dan Shim for useful comments on Rietveld analyses. Comments by two anonymous reviewers helped in improving the manuscript. Preliminary experiments were conducted at HPCAT, APS, Argonne National Laboratory with the help of Yue Meng. This work was performed at GSECARS, APS, Argonne National Laboratory. GSECARS is supported by the NSF, DOE, and the state of Illinois. Use of the APS was supported by the DOE, Office of Science, Office of Basic Energy Sciences.

References

Akahama, Y., H. Kawamura, and A. K. Singh (2002), Equation of state of bismuth to 222 GPa and comparison of gold and platinum pressure scales to 145 GPa, *J. Appl. Phys.*, *92*, 5892–5897.

Akaogi, M., H. Kojitani, H. Yusa, R. Yamamoto, M. Kido, and K. Koyama (2005), High-pressure transitions and thermochemistry of $MGeO_3$ (M = Mg, Zn, and Sr) and Sr-silicates: Systematics in enthalpies of formation of $A^{2+}B^{4+}O_3$ perovskites, *Phys. Chem. Miner.*, *32*, 603–613.

Anderson, D. L., and O. L. Anderson (1970), Bulk modulus-volume relationship for oxides, *J. Geophys. Res.*, *75*, 3494–3500.

Caracas, R., and R. E. Cohen (2005), Prediction of a new phase transition in Al2O3 at high pressures, *Geophys. Res. Lett.*, *32*, L06303, doi:10.1029/2004GL022204.

Hammersley, A. P., S. O. Svensson, M. Hanfland, A. N. Fitch, and D. Häusermann (1996), Two-dimensional detector software: From real detector to idealized image or two-theta scan, *High Pressure Res.*, *14*, 235–248.

Hirose, K., K. Kawamura, Y. Ohishi, S. Tateno, and N. Sata (2005), Stability and equation of state of $MgGeO_3$ post-perovskite phase, *Am. Mineral.*, *90*, 262–265.

Hohenberg, P., and W. Kohn (1964), Inhomogeneous electron gas, *Phys. Rev.*, *136*, B864–B871.

Holmes, N. C., J. A. Moriarty, G. R. Gathers, and W. J. Nellis (1989), The equation of state of platinum to 660 GPa (6.6 Mbar), *J. Appl. Phys.*, *66*, 2962–2967.

Kavner, A., and T. S. Duffy (2003), Elasticity and rheology of platinum under high pressure and nonhydrostatic stress, *Phys. Rev. B.*, *68*, 144101.

Kresse, G., and J. Furthmüller (1996), Efficiency of ab-initio total energy calculations for metals and semiconductors using a plane-wave basis set, *Comput. Mater. Sci.*, *6*, 15–50.

Kresse, G., and J. Hafner (1993), Ab initio molecular dynamics for liquid metals, *Phys. Rev. B*, *47*, 558–561.

Kresse, G., and D. Joubert (1999), From ultrasoft pseudopotentials to the projector augmented-wave method, *Phys. Rev. B.*, *59*, 1758–1775.

Larson, A. C., and R. B. Von Dreele (1994), General Structure Analysis System (GSAS), *Rep. LAUR 86–748*, Los Alamos Natl. Lab., Los Alamos, New Mexico.

Liebermann, R. C. (1975), Elasticity of olivine (alpha), beta (beta), and spinel (gamma) polymorphs of germanates and silicates, *Geophys. J. R. Astron. Soc.*, *42*, 899–929.

Mao, W. L., G. Shen, V. B. Prakapenka, Y. Meng, A. J. Campbell, D. L. Heinz, J. Shu, R. J. Hemley, and H.-K. Mao (2004), Ferromagnesian postperovskite silicates in the D″ layer of the Earth, *Proc. Natl. Acad. Sci. U. S. A.*, *101*, 15,867–15,869.

Merkel, S., A. Kubo, L. Miyagi, S. Speziale, T. S. Duffy, H.-K. Mao, and H.-R. Wenk (2006), Plastic deformation of $MgGeO_3$ post-perovskite at lower mantle pressure, *Science*, *311*, 644–646.

Murakami, M., K. Hirose, K. Kawamura, N. Sata, and Y. Ohishi (2004), Post-perovskite phase transition in $MgSiO_3$, *Science*, *304*, 855–858.

Oganov, A. R., and S. Ono (2004), Theoretical and experimental evidence for a post-perovskite phase of $MgSiO_3$ in Earth's D″ layer, *Nature*, *430*, 445–448.

Ono, S., T. Kikegawa, and Y. Ohishi (2006), Equation of state of $CaIrO_3$–type $MgSiO_3$ up to 144 GPa, *Am. Mineral.*, *91*, 475–478.

Riggs, E. M., and H. W. Green II (2005), A new class of microstructures which lead to transformation-induced faulting in magnesium germanate, *J. Geophys. Res.*, *110*, B03202, doi:10.1029/2004JB003391.

Ringwood, A. E., and M. Seabrook (1963), High-pressure phase transformations in germinate pyroxenes and related compounds, *J. Geophys. Res.*, *68*, 4601–4609.

Ross, N. L., and A. Navrotsky (1988), Study of the $MgGeO_3$ polymorphs (orthopyroxene, clinopyroxene, and ilmenite structures) by calorimetry, spectroscopy, and phase equilibria, *Am. Mineral.*, *73*, 1355–1365.

Sato, Y., E. Ito, and S.–I. Akimoto (1977), Hydrostatic compression of ilmenite phase of $ZnSiO_3$ and $MgGeO_3$, *Phys. Chem. Miner.*, *2*, 171–176.

Shen, G., V. B. Prakapenka, P. J. Eng, M. L. Rivers, and S. R. Sutton (2005), Facilities for high-pressure research with the diamond anvil cell at GSECARS, *J. Synchrotron Radiat.*, *12*, 642–649.

Shieh, S. R., T. S. Duffy, A. Kubo, G. Shen, V. B. Prakapenka, N. Sata, K. Hirose, and Y. Ohishi (2006), Equation of state of the post-perovskite phase synthesized from a natural (Mg, Fe)SiO_3 orthopyroxene, *Proc. Natl. Acad. Sci. U. S. A.*, *103*, 3039–3043.

Shim, S.-H., T. S. Duffy, R. Jeanloz, and G. Shen (2004), Stability and crystal structure of $MgSiO_3$ perovskite to the core-mantle boundary, *Geophys. Res. Lett.*, *31*, L10603, doi:10.1029/2004GL019639.

Singh, A. K. (1993), The lattice strains in a specimen (cubic system) compressed nonhydrostatically in an opposed anvil device, *J. Appl. Phys.*, *73*, 4278–4286.

Stackhouse, S., J. P. Brodholt, J. Wookey, J.-M. Kendall, and G. D. Price (2005), The effect of temperature on the seismic anisotropy of the perovskite and post-perovskite polymorphs of $MgSiO_3$, *Earth Planet. Sci. Lett.*, *230*, 1–10.

Tateno, S., K. Hirose, N. Sata, and Y. Ohishi (2006), High-pressure behavior of $MnGeO_3$ and $CdGeO_3$ perovskites and the post-perovskite phase transition, *Phys. Chem. Miner.*, *32*, 721–725.

Tsuchiya, T., J. Tsuchiya, K. Umemoto, and R. M. Wentzcovitch (2004), Phase transition in $MgSiO_3$ perovskite in the earth's lower mantle, *Earth Planet. Sci. Lett.*, *224*, 241–248.

Xia, X., D. J. Weidner, and H. Zhao (1998), Equation of state of brucite: Single-crystal Brillouin spectroscopy study and polycrystalline pressure-volume-temperature measurement, *Am. Mineral.*, *83*, 68–74.

R. J. Cava, Department of Chemistry, Princeton University, Princeton, NJ 08544, USA.

T. S. Duffy and A. Kubo, Department of Geosciences, Princeton University, Guyot Hall, Washington Rd., Princeton, NJ 08544–1003, USA. (akudo@princeton.edu)

B. Kiefer, Department of Physics, New Mexico State University, PO Box 30001, Las Cruces, NM 88003–8001, USA.

V. B. Prakapenka, CARS, University of Chicago, Argonne National Laboratory, 9700 S. Cass Ave., Bldg. 434, Argonne, IL 60439, USA.

G. Shen, HPCAT, Advanced Photon Source, Argonne National Laboratory, Building 401, 9700 S. Cass Avenue, Argonne, IL 60439, USA.